Available online at www.sciencedirect.com

ScienceDirect

Procedia Manufacturing 38 (2019) 1516–1523

Procedia MANUFACTURING

www.elsevier.com/locate/procedia

29th International Conference on Flexible Automation and Intelligent Manufacturing (FAIM2019), June 24-28, 2019, Limerick, Ireland.

Rheological Behaviour of PP Nanocomposites by Extrusion Process

F. De Almeida[a,b*], E. Costa e Silva[a,b], A. Correia[a,b], F. J. G. Silva[c]

[a] *ESTG – School of Management and Technology, Rua Curral, Rua do Curral - Margaride, 4610-156 Felgueiras, Portugal*
[b] *CIICESI – Center for Research and Innovation in Business Sciences and Information Systems - Margaride, 4610-156 Felgueiras, Portugal*
[c] *ISEP – School of Engineering, Polytechnic of Porto, Rua Dr. António Bernardino de Almeida, 431, 4249-015 Porto, Portugal*

Abstract

The effect of organophilic clay (C15A) in PP compatibilized polymer (PP/PP-g-MA) through rheological experimental results is presented. This study focusses on the description of the rheological behaviour of the organophilic layers along the screws of a twin screw extruder by melting process, varying the screw profile as well as the processing conditions, namely screw speed, temperature and feed rate. Different levels of dispersion were found along the screws for all conditions and positions analyzed by rheology. The qualitative analysis of the images obtained by transmission electron microscopy, reinforced the results. Furthermore, the effects of the processing conditions on dispersion of C15A layers along the screw profile are analyzed using multiple linear regression techniques. The results show statistically significant differences of all rheology measures for all the processing conditions and positions along the extruder.

Keywords: Rheology, Nanocomposites; Twin Screw Extruder; Processing Conditions; Multiple Linear Regression.

1. Introduction

The integration of organophilic silicate layers (OMMTs) into a polymer matrix strongly affects the rheological behaviour that, in turn, may improve the overall performance of the resulting (nano)composite. The remarkable effect of these nanolayers on the rheological properties of polymer systems has required special attention from researchers [1-4] and it is associated, mainly, with the high aspect ratio of the layers, that induces percolation and network formation under low filler concentration [4-9].

10.1016/j.promfg.2020.01.135

Given its engineered properties, organoclay/polypropylene (OMMT/PP) nanocomposites are attractive in developing novel components of interest in several fields of application [1-3,10]. To reach the percolation and network formation, a functionalized polypropylene is generally used as a compatibilizer to prepare PP nanocomposites. Chemically, there are two important factors affecting the nanocomposites formation: the miscibility of the compatibilizer with the bulk polymer and its concentration in the PP/compatibilizer/organoclay system [11-13]. A compatibilizer, promoting the adhesion between the polymer matrix and the layers, induces both better intercalation of the macromolecules and an increase of the interfacial surface. This supports exfoliation or dispersion mechanisms that gives rise to higher dynamic components values at low frequencies.

Several important works concerning the end of the extrusion process exist. The works by [14-17] concentrate on the optimization properties of an OMMT-loaded polymer composite and the rheological behaviour, which is of great importance to analyze the performance of nanocomposite material produced by processing techniques, is explored in [4,11,14,17]. Considering the nanosized of the layers, a complementary technique such as transmission electron microscopy (TEM) is required [17-19]. The main conclusions are that the structure of the organophilic clay layers depends on the attributes of the polymer matrix and of the clay, but also depends on the operating conditions during processing. Processing of polymer nanocomposites by melting techniques, such as extrusion, requires sufficient stress levels and time for a maximum exfoliation/intercalation of the organoclays silicate layers (with minimum polymer degradation) to ensure adequate nanometric dispersion [12,13,17]. It consists of using a twin-screw extruder (TSE) as a continuous process.

The problem of determining the processing conditions to ensure adequate nanometer dispersion into a polymer remains a real challenge. The necessary information with the required precision is sometimes difficult to obtain. In order to demystify this question, a new approach is applied by studying the rheological behaviour.

After a general presentation of the effect of different processing conditions of the produced PP (nano)composites at die outlet [14], this study will focus on the dispersion attained in the continuous process along the processing path by analysing the rheological curves, for the selected conditions. The PP (nano)composites were obtained by compounding, using a TSE of a PP/PP-g-MA/C15A system. The effect of both, the screw intensity and the extrusion parameters (i.e. screw rotational speed, temperature and flow rate) on the C15A layers dispersion of melt-mixed PP/clay nanocomposites at 9.5, 11 e 32 L/D were investigated. The evaluation of the dispersion degree was obtained from the dynamic rheological measurements: storage modulus (G'), loss modulus (G'') and complex viscosity ($|\eta^*|$). Rheology indicates different levels of silicate layers/aggregate (or tactoide structures) of C15A along the screws profiles, observed in the TEM images. Those aggregates indicate some rearrangement of the organophilic layers during the extrusion process. The demonstrated dispersion of the nanolayers is attributed to sufficient local shear rate and residence time. Using linear multivariate models for the rheological measurements G', G'' and $|\eta^*|$, the optima procession conditions are suggested.

2. Methodology

A mixture of 5 wt. % loading of the organoclay Cloisite 15A (C15A), a powder with an average particle size of 8 μm, 15 wt.% of the PP modified, with 1 % of maleic anhydride (PP-g-MA), and 80 wt.% of the polypropylene (PP) pellets, were premixed in a tumbler. Experimental studies of melting the organophilic layers C15A into PP/PP-g-MA were carried out on a Leistritz 34 mm modular intermeshing co-rotating TSE, according to the screw configurations used in [14]. The screws are 29D long and contain different mixing zones with Kneading Disc (KD) staggered and left-end element, which can be made up of different width paddles. The wider the paddle, the more elongational shear and dispersive mixing is induced [12,13,17]. Since high shear intensity screw profile is required to enhance dispersion, the sampling devices are located on these regions where positive pressure is developed (Fig. 1). Then, samples of material were quickly removed from the extruder and frozen in liquid nitrogen, before any morphology evolution took place, for subsequent offline characterization.

The angles of KD included in the screws of 90º and -30º, increase the intensity of the screws profile, considered as the low (P1) and high (P2) screw intensity, respectively. The parameters screw speed (150 rpm – N1 and 300 rpm – N2), temperature (170 ºC – T1, 180 ºC – T2 and 190 ºC – T3) and feed rate (2 $kg{\cdot}h^{-1}$ – Q1, 4 $kg{\cdot}h^{-1}$ – Q2 and 6 $kg{\cdot}h^{-1}$ – Q3), were also studied along the TSE at 9.5 L/D, 11 L/D and 32 L/D (Fig. 1), by varying each one independently.

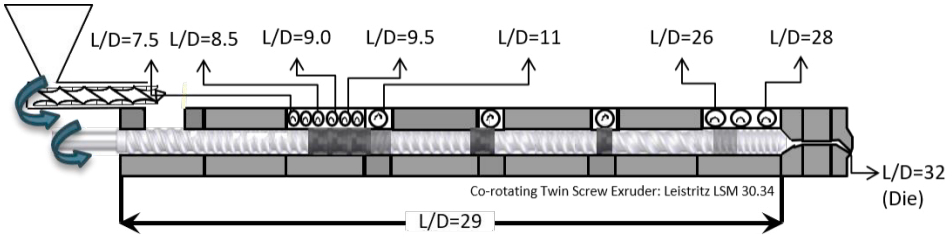

Fig. 1. Extruder layout of TSE and sampling devices.

The oscillatory experiments were performed on the oscillatory rheometer with parallel-plate geometry. From these experiments, the dynamic response of the material was performed in linear viscoelastic properties (5% of strain). G', G'' and |η*| performance of the C15A in the compatibilized PP, with oscillation frequencies from 0.1 to 10 Hz were investigated. Note that, since the samples of material are taken from the sampling devices along the extruder, their removal from the inside the extruder is quickly. The dynamic components of PP/PP-g-MA loaded C15A was measured in a TA instruments RG2 oscillatory rheometer with isothermal frequency sweeps at 195ºC from 0.01 to 100 rad·s^{-1}. Furthermore, samples for TEM analysis were cryosectioned at a thickness under 90 nm with a cryo-ultramicrotome at -45 ºC and examined using a JEOL-JEM 1010 Transmission Electron Microscope (operating with a voltage of 100 kV).

In the present work, the results obtained by experimental techniques on the formation of PP/PP-g-MA/C15A nanocomposites were used to test the existence of significant differences between the dispersion results for different processing conditions and positions along the screw

2.1. Experimental Results

Rheological curves for PP and G' results for the PP/PP-g-MA/C15A at different positions along the P1 screws configuration, holding a constant feed rate of 4 kg·h^{-1}, temperature of 180 °C, and a screw speed of 300 rpm (Fig. 2). All the dynamic curves (G', G'' and |η*|) of the PP nanocomposites are similar to the left curves (typical presentation) (Fig. 2), only an increase of components at low frequencies is observed in the presence of the organoclays C15A, as can seen by G' results (Fig. 2, right). Comparing PP with the dynamic response of OMMT-based nanocomposite at 9.0, 9.5, 11, 26 and 32 L/D (die), as expect [4-9], the use of organophilic layers generate good interfacial properties indicative of the higher value of G' for all positions (Fig. 2) which confirms a network formation. The same behaviour has been found on G'' and |η*|. Generally, it means that the required specific interactions between the polymer chains

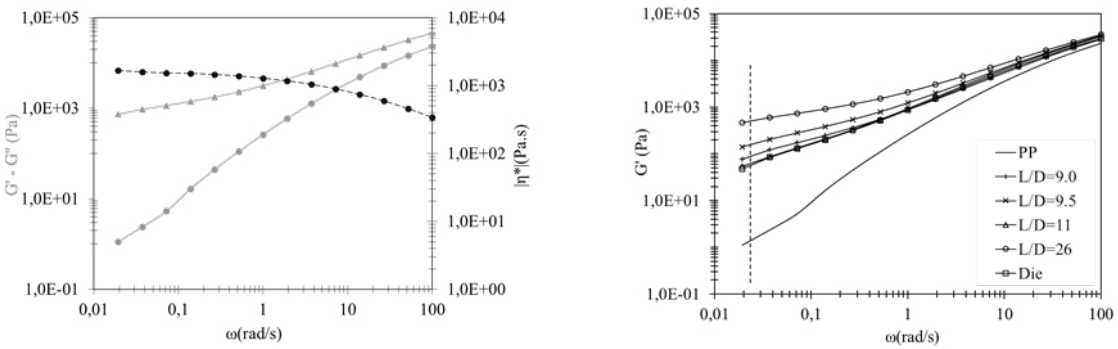

Fig. 2. Typical dynamic curves of storage modulus (G'), loss modulus (G'') and complex viscosity (|η*|) for PP (left) and G' results at 9.0, 9.5, 11, 26 L/D and die for PP nanocomposite (right).

and the surfaces of the organophilic layers have been established so that the dispersion of the organophilic layers of

the obtained nanocomposites occurred [1-3,10]. Furthermore, assorted levels of dispersion along the screw seem to exist, with the highest degree at 26 L/D.

Research on this topic has been focused on bulk rheological properties at die outlet [11,12,14,16,17], while in the present paper the dynamic experiments to explore the evolution along the screw profile, when PP compatibilized is loaded with the organoclay C15A, was employed. In Fig. 3, the PP/PP-g-MA/C15A nanocomposites values of G' response to the polymeric PP/PP-g-MA at 0.02 rad·s^{-1} can be compared. In general, the incorporation of C15A layers and modified PP have altered the magnitude of the G' dynamic components at low frequencies. The rheological results - G', G'' and |η*| - suggested that the intercalation and exfoliation of nanoparticles could be achieved by TSE process, which is generally governed by the matrix viscosity. Although a decrease of dispersion and network formation is mostly presented at 11L/D, in this position it was not possible to produce high levels of dispersion. These results seem to indicate that the attractive forces between the layers become dominant and therefore promoting its re-aggregation [7-9], probably due to the highest shear rate (and cumulative residence time) that the material was subject. Moreover, some evolution is observed at 32 L/D. After the higher stresses applied, the appropriate mechanical shear relaxation movement (during shorter periods with a lower number of KD) can again promote intercalation and exfoliation of the layers and the dispersion reversion seems to be induced. Finally, higher levels of dispersion were identified at die (32 L/D) for P2N1, P2T1 and P2Q3 conditions, as consequence of the studied effect of screw speed and profile, temperature and feed rate, respectively.

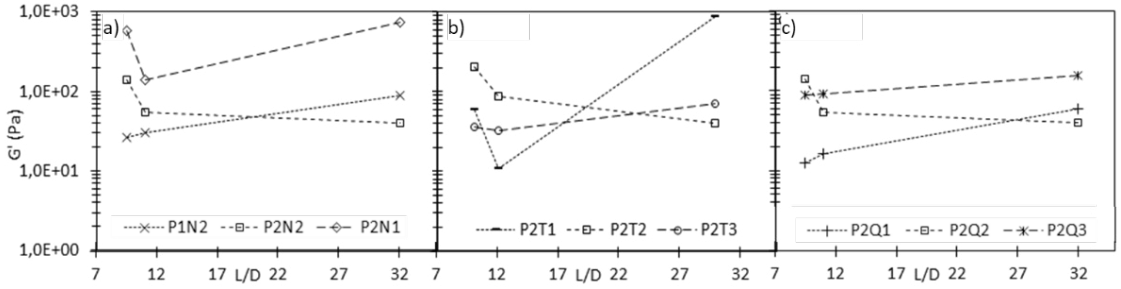

Fig. 3. G' results for different screw profile and speed (a), temperature (b) and feed rate (c) of PP/PP-g-MA/C15A at 9.5, 11 and 32 L/D.

The microstructure was evaluated by microscopy along the extruder at 9.5, 11 and 32 L/D, and for the selected processing conditions (Fig. 4), where P2X2 is the transversal condition. To analyse the effect of the profile and the screw speed, X is replaced by N, meaning that the results are compared to the conditions labelled as P1N2, P2N1 and P2N2. To study the effects of temperature, X is replaced by T, while for feed rate X is replaced by Q.

Quality control has demanded methods to quantify the mixing state of nanolayers embedded in polymeric materials. TEM images of the PP/PP-g-MA/C15A nanocomposite revealed a general well-exfoliated structure but also revealed a partial exfoliation along with areas containing exfoliated platelets and unintercalated tactoids. This was in good agreement with data obtained in G', G'' and |η*| evaluations. For the highest intensity (P2) at 11L/D, a decrease of exfoliated layers was observed, namely: P2N1, P2X2, P2T1 and P2T3. Again, higher levels of exfoliation and dispersion were observed at 32 L/D (Die) for P2N1, P2T1 and P2Q3. This highest levels of intercalation and exfoliation of the C15A layers at the end of the process were observed for samples produced with intense screw profile (P2) and with lower screw speed (N1), lower temperature (T1) and high feed rate (Q3). Thus, results confirm the higher intensity screw profile required to break up the tactoid structure of the C15A layers along the extruder. The extent of exfoliation appears to be strongly affected by the mixing conditions, while the degree of dispersion is generally governed by the average shear rate and the mixing time [17]. High levels of dispersion of layers agglomerates seems not be achieved when the cohesive forces of the agglomerates are exceeded by the hydrodynamic separating forces applied by the fluid polymer with longer mixing time, as occurs at 11L/D in the end of the first mixing block (Fig.1). For that, it seems to occur reversion of exfoliation or dispersion of the C15A layers with a partial collapse of the network structure formed. The described results show the need to deepen the behaviour of the material during the extrusion process.

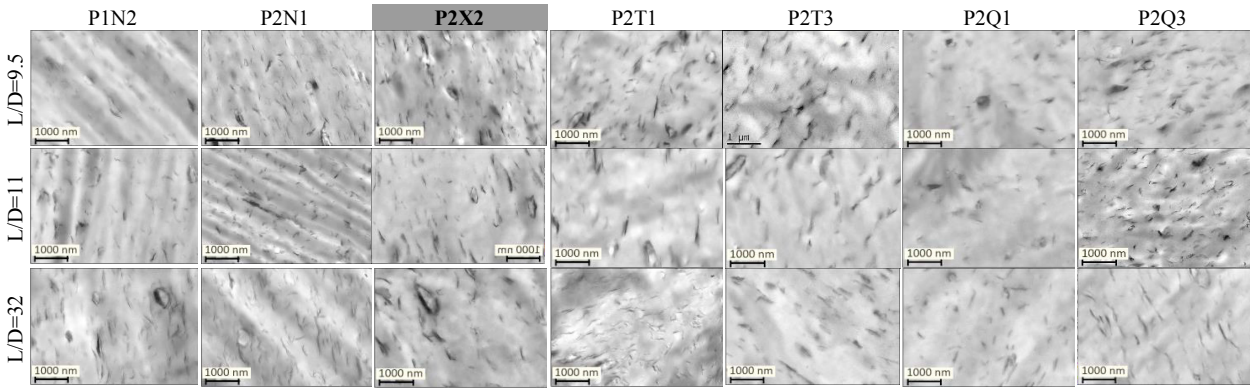

Fig. 4. TEM images of PP/PP-g-MA/C15A for different screw intensity and screw speed (P1N2, P2N1 and P2N2), temperature (P2T1, P2T2, P2T3) and feed rate (P2Q1, P2Q2 and P2Q3) at 9.5, 11 and 32 L/D.

2.2. Statistic Results

In this paper, the dynamic rheological measurements of the C15A layers dispersion along the extruder are also studied statistically. A total of 19 experiments are available for 9.5 L/D (reference class), and 17 experiments for 11 L/D and 32 L/D. The location is, therefore, a qualitative variable. Concerning the processing conditions, the reference classes are: high profile (P2), screw speed of 300 rpm (N2), temperature of 180 ºC (T2) and feed rate of 4 kg·h^{-1} (Q2). Furthermore, the angular frequency (ω) is a quantitative variable ranging from 0.01 rad·s^{-1} to 1 rad·s^{-1}, considering the region of interest [11-13].

For each dynamic rheological measurement G', G'' and $|\eta^*|$, a multiple linear regression model is estimated. The logarithm transformation is applied to the dependent variables G', G'' and $|\eta^*|$ and to the independent variable angular frequency.

Table 2 presents the estimates and validation of the models for each of the three dynamic rheological measurements. Analyzing the behaviour of the residuals (see Figs. 5-7), we can conclude that, for all models, the residuals are randomly distributed around zero ranging approximately from -2 to 2. The residuals present similar behaviour to a normal distribution, although with slight deviations on the tales. The leverage values are less than 0.031, thus there is no evidence of the existence of outliers. The maximum value for VIF (variance inflation factor) is 2.2844. From Table 2, the estimated model for G' (Eq. 1) is:

$$\log(G') = 7.06704 + 0.73843\log(\omega) - 0.37058\,\mathrm{P1} + 1.18244\,\mathrm{N1} - 0.27866\,\mathrm{T1} - 0.98451\,\mathrm{T3}$$

$$-1.93934\,\mathrm{Q1} + 0.26959\,\mathrm{Q3} - 0.52368\,LD[11] + 0.69186\,LD[32] \quad (1)$$

All processing conditions are statistically significant, for a significant level of 1%, to G'. For any 10% increase in frequency, the expected ratio of G' will be $1.10^{0.73843} \approx 1.07$, i.e. it is expected a 7% increase in G' when the frequency increases by 10%, keeping the other variables constant. The expected percentage decrease in the geometric mean from high to low profile is approximately 31%, keeping the other variables constant since $\exp(0.37058) \approx 0.69$. The expected percentage increase in geometric mean from a speed of 300 rpm to 150 rpm is approximately 226 %, keeping the other variables constant, since $\exp(1.18244) \approx 3.26$. For a decrease in temperature from 180 ºC to 170 ºC, and for an increase in temperature from 180 ºC to 190 ºC, there is an expected percent decrease in the geometric mean of G' of 24% and 63%, respectively, holding the other variables constant. Relatively to the feed rate (Q) it can be stated that when it decrease from 4 kg·h^{-1} to 2 kg·h^{-1} there is an expected percent decrease in the geometric mean of G' of 86% $(1 - \exp(-1.93934) \approx 0.86)$, holding the other variables constant. While an increase of the Q from 4 kg·h^{-1} to 6 kg·h^{-1} has as consequence an expected percentage increase in the geometric mean of G' of 31% $(\exp(0.26959) \approx 1.31)$, holding the other variables constant. In terms of the position along the TSE, G' at 11 L/D, when compared to 9.5 L/D and holding the other variables constant, presents a decrease in the geometric mean of 41% $(1 - \exp(-0.52368) \approx 0.41)$. At the die, i.e. 32 L/D, there is an increase of the geometric mean of 100% $(\exp(0.69186) \approx 2.00)$, when compare to G' at 9.5 L/D.

The above results suggest that the storage modulus, G', is maximal for high profile, speed of 150 rpm, 180 ºC of temperature, feed rate of 6 kg.h^{-1} and at 32 L/D. Considering the discussion in the section 2.1. unexpected results were found related to the temperature. For G'' and |η*|, the estimated models are in (Eq. 2) and (Eq. 3), respectively:

$$\log(G'') = 7.71584 + 0.74133\log(\omega) - 0.14928\text{P1} + 0.62193\ \text{N1} - 0.05203\ \text{T1} - 0.58651\text{T3}$$
$$-0.7873\ \text{Q1} + 0.04836\ \text{Q3} - 0.21980\ LD[11] + 0.33092\ LD[32] \quad (2)$$

$$\log(|\eta*|) = 7.818089 - 0.28187\log(\omega) - 0.19856\ \text{P1} + 0.81676\ \text{N1} + 0.00258\ \text{T1} - 0.66069\ \text{T3}$$
$$-0.90718\ \text{Q1} + 0.09384\ \text{Q3} - 0.27897\ LD[11] + 0.40658\ LD[32] \quad (3)$$

Table 1: Estimates and model validation.

Dependent variables	log (G')		log (G")		log (|η*|)	
Independent variables	Estimate	p-value	Estimate	p-value	Estimate	p-value
(Intercept)	7.06704	< 2.00e-16***	7.71584	< 2.00e-16***	7.81089	< 2.00e-16***
log (ω)	0.73843	< 2.00e-16***	0.74133	< 2.00e-16***	-0.28187	< 2.00e-16***
P1	-0.37058	0.002**	-0.14928	0.013*	-0.19856	0.007**
N1	1.18244	< 2.006-16***	0.62193	< 2.00e-16***	0.81676	< 2.00e-16***
T1	-0.27866	0.028*	-0.05203	0.41	0.00258	0.974
T3	-0.98451	2.86e-13***	-0.58651	< 2.00e-16***	-0.66069	2.70e-15***
Q1	-1.93934	< 2.00e-16***	-0.78730	< 2.00e-16***	-0.90718	< 2.00e-16***
Q3	0.26959	0.033*	0.04836	0.442	0.09384	0.227
L/D=11	-0.52368	3.83e-10***	-0.21980	1.12e-07***	-0.27897	5.25e-8***
L/D=32	0.69186	5.26e-16***	0.33092	6.28e-15***	0.40658	8.88e-15***
Signif. codes: 0 '***' 0.001 '**' 0.01 '*' 0.05 '.' 0.1 ' ' 1						
Adjusted R-squared	0.8193		0.9244		0.7266	
ANOVA						
F-statistic	214.1 on 9 and 414 DF		575.3 on 9 and 414 DF		125.9 on 9 and 414 DF	
p-value	< 2.2e-16		< 2.2e-16		< 2.2e-16	

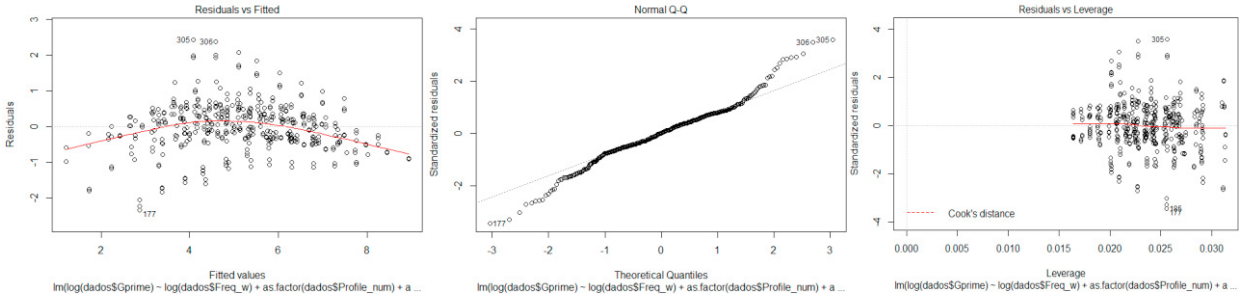

Fig. 5. Residual analysis for G'

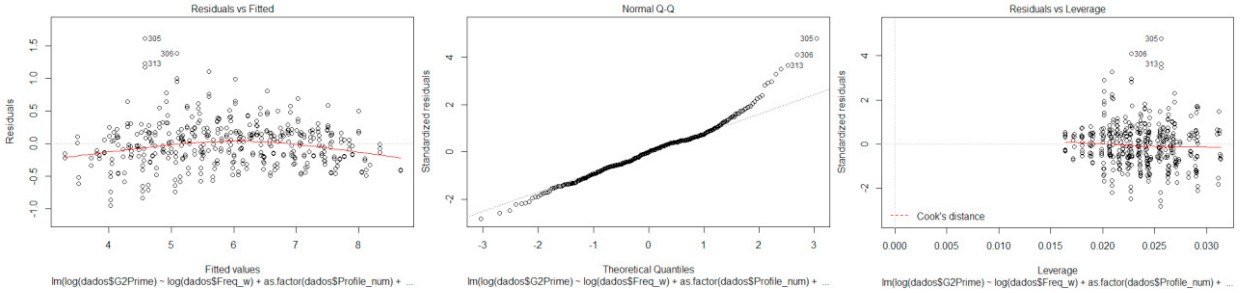

Fig. 6. Residual analysis for G''

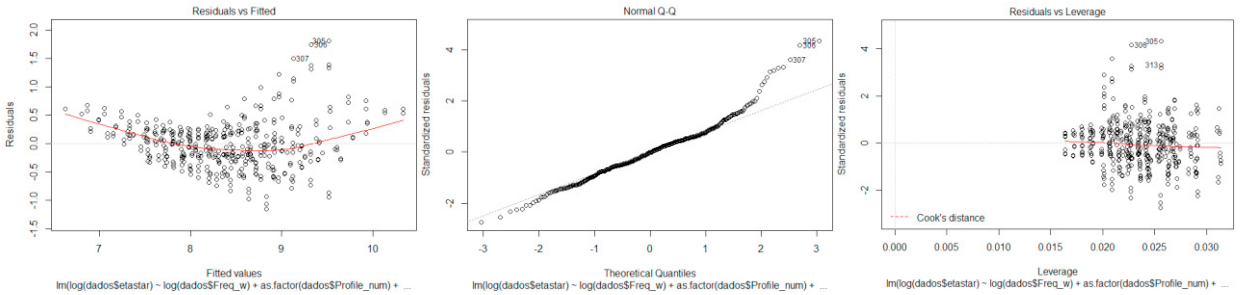

Fig. 7. Residual analysis for |η*|

The obtained results for feed rate and temperature in these models are not statistically significant for all classes. There are no differences between the experiments when the feed rate decreases from 4 to 2 kg.h^{-1} and temperature decreases from 180 to 170 ºC.

Similarly to the previous analysis, the models suggest that the loss modulus, G'', and complex viscosity, |η*|, are highest for high profile, 150 rpm screw speed, 170 ºC or 180 ºC temperatures, 4 or 6 kg·h^{-1} feed rate and at 32 L/D. The models indicate that, for the intense screw profile (P2), the favourable conditions that would probably increase the degree of dispersion and exfoliation. However, the condition was not tested experimentally, which is an opportunity for future work.

3. Conclusions

In this work, the effect of processing conditions, namely screw profile and speed, temperature and feed rate, along the screw axis (9.5, 11 and 32 L/D) of a TSE on exfoliation/dispersion of C15A layers in PP/PP-g-MA is firstly studied through the offline characterization of samples (rheological and microscopy analyses). The melt viscosity of OMMT-based nanocomposites increased, which contributes towards improving clay dispersion. Along with the correct chemistry, the level of shear stress transfer from the polymer matrix to the clays needs to be high, and intense screw profile (P2) has imposed larger levels of dispersion. Results of various processing conditions in a twin screw extruder showed that shear stress and longer residence time could change the morphology leading to some reversion of the clay dispersion with lowest values of the dynamic components at 11 L / D. Furthermore, the effects of the processing conditions on the dispersion of C15A layers are analyzed using multiple linear regression techniques. The results show statistically significant differences in all rheology measures for all the processing conditions and positions along the extruder. The obtained model for the storage modulus, suggest that G', is maximal for high profile, speed of 150 rpm, 180 ºC of temperature, feed rate of 6 kg.h^{-1} and at 32 L/D. Similarly, the models suggest that the loss modulus, G'',

and complex viscosity |η*| are maximal for high profile, speed of 150 rpm, 170 ºC or 180 ºC of temperature, feed rate of 4 or 6 $kg.h^{-1}$ and 32 L/D.

More than verifying and generalize these results, the statistical models allow to identify at the end of the extrusion process, i.e. 32 L/D, which are the favourable conditions that enlarged the dispersion of organophilic layers of the C15A for the high screw profile used.

References

[1] Y. Dong, A. Pramanik, D. I. Liu and R. Umer, Manufacturing, Characterisation and Properties of Advanced Nanocomposites, Journal Composites, (2018). ISBN 978-3-03897-189-4.

[2] M. J. Mochane, T. C. Mokhena, T. H. Mokhothu, A. Mtibe, E. R. Sadiku, S. S. Ray, The Importance of Nanostructured Materials for Energy Storage/Conversion, In Handbook of Nanomaterials for Industrial Applications. Micro and Nano Technologies, (2018) 768–792.

[3] J. Gonçalves, P. Lima, B. Krause, P. Pötschke, U. Lafont, J. R. Gomes, C. S. Abreu, M. C. Paiva, J. A. Covas, Electrically Conductive Polyetheretherketone Nanocomposite Filaments: From Production to Fused Deposition Modeling, Polymers, 10 (2018) 1–20.

[4] S. Cho, J. S. Hong, S. J. Lee, K. H. Ahn, J. A. Covas, J. M. Maia, Morphology and rheology of polypropylene/polystyrene/clay nanocomposites in batch and continuous melt mixing processes, Macromolecular Materials and Engineering, 296 (2011) 341–348.

[5] P. Cassagnau, Melt rheology of organoclay and fumed silica nanocomposites, Polymer, 49 (2008) 2183–2196.

[6] S. Yu, S. Liu, J. Zhao, M. S. Yong, Study of rheological properties of polypropylene/organoclay hybrid materials, Journal Nanoscience Nanotechnology, 6 (2006) 89–92.

[7] R. Krishnamoorti, E. P. Giannelis, Rheology of End-Tethered Polymer Layered Silicate Nanocomposites, Macromolecules, 30 (1997) 4097–4102.

[8] J. Ren, B. F. Casanueva, C. A. Mitchel, R. Krishnamoorti, Disorientation Kinetics of Aligned Polymer Layered Silicate Nanocomposites. Macromolecules, 36 (2003) 4188–4194.

[9] L. Xu, H. Nakajima, E. Manias, R. Krishnamoorti, Tailored Nanocomposites of Polypropylene with Layered Silicates. Macromolecules, 42 (2009) 3795–3803.

[10] J. W. Gilman, Flammability and thermal stability studies of polymer layered-silicate clay nanocomposites, Applied Clay Science, 15 (1999) 31–49.

[11] G. Normand, A. Mija, S. Pagnotta, E. Peuvrel-Disdier, B. Vergnes, Preparation of polypropylene nanocomposites by melt-mixing: Comparison between three organoclays, Journal of Applied Polymer Science, 134, 45053 (2017) 2-8.

[12] Y. Yoo, D. R. Paul, Effect of organoclay structure on morphology and properties of nanocomposites based on an amorphous polyamide, Polymer, 49 (2008) 3795−3804.

[13] T. Domenech, E. Peuvrel-Disdier, B. Vergnes, The importance of specific mechanical energy during twin screw extrusion of organoclay based polypropylene nanocomposites, Composites Science and Technology, 75 (2013) 7−14.

[14] M. F. De Almeida, A. Correia, E. Costa e Silva, Layered clays in PP polymer dispersion: the effect of the processing conditions. Journal of Applied Statistics, 45 (2018) 558–567.

[15] T. Villmow, P. Pötschke, S. Pegel, L. Häussler, B. Kretzschmar, Influence of twin-screw extrusion conditions on the dispersion of multi-walled carbon nanotubes in a poly (lactic acid) matrix, Polymer, 49 (2008) 3500–3509.

[16] W. Lertwimolnun, B. Vergnes, Effect of processing conditions on the formation of polypropylene/organoclay nanocomposites in a twin screw extruder, Polymer Engineering & Science, 46 (2006) 314–323.

[17] H. Dennis, D. L. Hunter, D. Chang, S. Kim, J. L. White, J.W. Cho, D. R. Paul, Effect of melt processing conditions on the extent of exfoliation in organoclay-based nanocomposites, Polymer, 42 (2001) 9513–9522.

[18] Z. P. Luo, J. H. Koo, Quantification of the layer dispersion degree in polymer layered silicate nanocomposites by transmission electron microscopy, Polymer, 49 (2008) 1841–1852.

[19] D. J. Carastan, A. Vermogen, K. Masenelli-Varlot, N. R. Demarquette, Quantification of clay dispersion in nanocomposites of styrenic polymers, Polymer Engineering & Science, 50 (2010) 257–267.